A CMOS CONDUCTOMETRIC CIRCUIT FOR CHEMICAL SENSING USING NANOWIRE SENSOR ARRAYS

by

SUJITH S DERMAL

Presented to the Faculty of the Graduate School of
The University of Texas at Arlington in Partial Fulfillment
of the Requirements
for the Degree of

MASTER OF SCIENCE IN ELECTRICAL ENGINEERING

THE UNIVERSITY OF TEXAS AT ARLINGTON

August 2013

Acknowledgements

First and foremost, with immense gratitude, I would like to acknowledge the support and help of my advisor, Dr. Sungyong Jung. I am indebted to him for his guidance and continuous support of my master's study and research, and for his patience and motivation. I have learnt a lot about research and its principles from him over this period, which will always be with me throughout my life along with his friendship.

I would also like to thank Dr. Kambiz Alavi and Dr. Ali Davoudi for being my thesis defense committee members. I want to mention the electrical engineering department assistants Ann and Janice for their constant and kind assistances.

I would like to thank my fellow former/current AMIC lab members: Varun, Niranjan and Sunil for all their invaluable inputs to my research and for being good friends to help create a great environment for research and discussions in the lab. Also I would like to thank my friends Nayana, Shiju, Sarath and Akhil. You all add so many positive things and great memories into my experiences.

Finally and most importantly, this thesis would not be possible without the love and support of my family and friends. My parents, my sister and my brother-in-law are my biggest strength and I thank them from the bottom of my heart and dedicate this work to them.

August 8, 2013

Abstract

A CMOS CONDUCTOMETRIC CIRCUIT FOR

CHEMICAL SENSING USING

NANOWIRE SENSOR ARRAYS

Sujith S Dermal, M.S.

The University of Texas at Arlington, 2013

Supervising Professor: Sungyong Jung

In this thesis, a readout circuit for conductometric electrochemical sensor array is designed and implemented. It is designed to work with the output range of a Carbon Nanotube Chemiresistive Sensor Array. The sensor arrays are designed to measure the Volatile Organic Compounds (VOCs) in the environment. The circuit reads out the outputs of the sixteen conductometric sensor arrays and calculates the change in conductance during the interaction with the chemicals present in the environment. A constant voltage is applied to the sensor arrays and when the sensor detects the VOCs, it changes the conductance and a change in current through the sensor arrays is observed. This change in current is measured by the readout circuit and the conductance can be found out. The conductometric circuit consist a 16:1 analog multiplexer, trans-impedance amplifier (TIA), and a microcontroller to control and process the signals.

For the CMOS IC implementation, the conductometric circuit is designed and fabricated in 0.35 um CMOS process. The design and analysis of the individual circuit components including the analog multiplexer and operational amplifier are presented in this work. The op amp achieves 118.1 dB gain and 59.79 degree phase margin. The circuit gives a linear dc response for the resistance variation range of 10 KΩ to 100 KΩ.

Table of Contents

List of Illustrations

List of Tables

Chapter 1

Introduction

Today we face a critical condition in the world relating to industrial pollution and other emissions which has led to the breakdown of ecosystems and human health. As processed building materials, plastics, household chemicals and automobiles became common, so did their chemical out gassing which includes volatile organic compounds (VOCs) [1]. Defined as organic compounds with vapor pressures >0.1 mm Hg at 25 °C and 760 mm Hg, VOCs have been found to cause many adverse health effects including respiratory distress, eye and throat irritation, neurological symptoms (e.g. fatigue, headaches and depression) and cancers [2,3,4].

VOCs found in ambient air have raised concerns also because of their contribution to the formation of other pollutants, including tropospheric ozone. The potential effects of a global increase in ozone (O_3) and other photochemical oxidants are far-ranging. Ozone is a source of hydroxyl (OH) radicals which reacts rapidly with most air pollutants, leading to the formation of VOCs linked to air contaminants. Because both O_3 and certain VOCs are greenhouse gases, this chemistry has implications for global climate change. Polycyclic aromatic hydrocarbons (PAHs) are ubiquitous in our air environment in which some are carcinogenic VOCs and they are the result of incomplete combustion of mobile (such as diesel and gasoline engine exhausts), stationary (such as coal-fired, electricity generating power plants), domestic (such as environmental tobacco smoke and residential wood or coal combustion), and area sources (such as forest fires and agricultural burning) [5]. In concerns for public safety, quantification and detection of ethanol vapors in breath is required for drivers under the influence of alcohol. In medical diagnosis, air exhaled by patients may be used to indicate lung cancer by identifying and quantifying various VOCs. Also uncontrolled diabetes is indicated by a sweet, fruity odor

due to excess acetone vapor in the breath [6]. High accuracy and sensitivity measurement and analysis of exposure are critical in correlating problems with health and environment to certain VOCs. Hence vapor sensing is required in a number of applications that range from medicine to environmental pollution.

Since the beginning of twentieth century, scientists from biology, chemistry and electrical field have been trying to analyze the electrical properties that results from chemical reactions in different types of biochemical sensor systems. The reason behind this is because it helps scientists and engineers to understand how the electrochemical sensors work with harmful chemical particles, how many harmful particles are present and how the agent controls can remove or reduce the harmful chemical particles. It also helps to diagnose and treat the problems related to health and environment in an efficient way. This particular capability of the electrochemical sensor has attracted the attention of both academia and industry which led to the research and development of several types of electrochemical sensors for the sensing of different chemical/biological agents. One of the main approaches to characterize the issues with VOCs is the analysis of electrical data from the gas sensors. The electrical data captured by these sensors provides medical doctors and engineers the ability to study the diseases or determine how the gases affect the environment. The characterization of gases from the gas sensing system provides the ability to determine how a gas sensor behaves and which sensor is more sensitive when exposed to certain dangerous gases.

Although a number of chemical sensors are commercially available for field measurements of chemical species, few have been adapted for use in geologic environments for long-term monitoring or remediation applications [7]. Electrochemical sensors are well-established and powerful tools to gain real-time information for process control by *in situ* measurements of chemical composition without sampling. As compared

to spectrometric, mass spectrometric and chromatographic techniques, electrochemical sensor systems are simple in their setup as well as in the electronic equipment necessary for operation and for data acquisition. The effort for maintenance and calibration is low. Therefore, they are preferred tools in industrial application and for screenings in field application [8].

Electrochemical sensors have been categorized by Wilson et al. (1995, Ch. 36) and Janata (1992) into three groups: (1) potentiometric (measurement of voltage); (2) amperometric (measurement of current); and (3) conductometric (measurement of conductivity). Among these, conductometric types of sensors appear to be most relevant for detecting and monitoring VOCs. Conductometric sensors indicate a change in conductance of the transducer when it is exposed to chemicals. By measuring this change in conductance with the help of an electronic circuitry and signal processing unit, we could analyze the target chemical. The most common conductometric sensing is done using chemiresistive sensor as they are small, low power devices that have no moving parts and have good sensitivity to various chemicals. The disadvantage with chemiresistive sensor is that it may not be able to discriminate among unknown mixtures of chemicals [7]. To overcome this disadvantage a sensor array has been developed with surface modification of chemiresistor with a suitable guest molecule that enhances sensing performance [9].

The objective of this research work is to develop a standalone portable conductometric sensing system to interface the chemiresistive sensor array which would provide improvements in the sensing of different VOCs which act as toxic substances in the environment. The following requirements for this standalone system must be satisfied: dynamic range, size and on-the-go USB powered from PC, tablet or smart phone. Before going to delineate the sensing system for the conductometric sensor

arrays, a background study about chemical and electrochemical sensors has been provided. An analysis and comparison of conductometric, potentiometric and voltametric sensing methods were also performed and is explained in this thesis.

This thesis is organized into four chapters:

Chapter 1 presents the motivation for VOC sensing system with a background of problems related to the health and environment due to certain chemicals. The research objectives for this thesis are also described.

Chapter 2 provides a background study of chemical sensors, electrochemical sensing mechanisms, conductometric (resistive) chemical sensors, chemical sensor arrays and review of readout circuits for conductometric sensing.

Chapter 3 provides the design of a conductometric circuit for chemical sensing using Porphyrin – Functionalized Single-Walled Carbon Nanotube (SWNT) Chemiresistive Sensor Arrays. It first shows a printed circuit board (PCB) implementation of the proposed conductometric circuit sensing system done with commercial off-the-shelf (COTS) components. Then an integrated circuit implementation of the proposed circuit in 0.35 um CMOS process is discussed with simulation and measurement results.

Chapter 4 concludes this thesis with the contribution of this work and a set of future research objectives that can be conducted to improve the results of this thesis.

Chapter 2

Background

2.1 Review of Chemical Sensors

What are "chemical sensors" and why is there such interest in them? Chemical sensors are intended for measurement of concentrations of chemical substances of an organic or inorganic nature in liquid and gaseous media. There are two obvious sources for the formation of chemical sensor science as an independent field. One of these sources is the development of micro technologies, which stimulated a demand for sensing organs. The second source is a consequence of the evolution is about a growing need for mobile analyses and their instrumentation [10]. Chemical sensors have become an indispensable part of our technology driven society and can be found in chemical process, pharmaceutical, food, biomedical, environmental, security, industrial safety, clinical, and indoor monitoring applications to highlight a few. Like many fields in science, chemical sensors have benefited from the growing power of computers, integrated electronics, new materials, novel designs, and processing tools. Manifestation of such technological changes can be seen in the development of miniaturized, inexpensive, portable, and mass manufacturable chemical sensors capable of static and continuous measurements even in remote environments [11].

The term "chemical sensor" or "sensor" is used for a sensitive element that reacts directly to a change of concentration of a specific component in an analyzed mixture; in other words, one that generates a signal that in magnitude is functionally related to the concentration of the component being determined. Chemical sensors can operate on chemical principles, where the analytical signal arises because of a chemical reaction between the component being determined and a sensitive layer consisting of a specific chemical substance, or on physical principles, where physical parameters are

being measured: absorption or reflection of light in different regions of the spectrum, conductivity, mass with a change of concentration of the component being determined. An inherent part of a chemical sensor is a transducer or converter of the energy of chemical, biochemical, or physical processes, usually to an electrical signal, which in turn is transmitted to the appropriate electronic device for further processing. In many chemical sensors these working elements are separately situated, while in modern sensors, for example chemically sensitive field-effect transistors and, without question, in future sensors all of these elements, including the processor, will be combined into a single device [12].

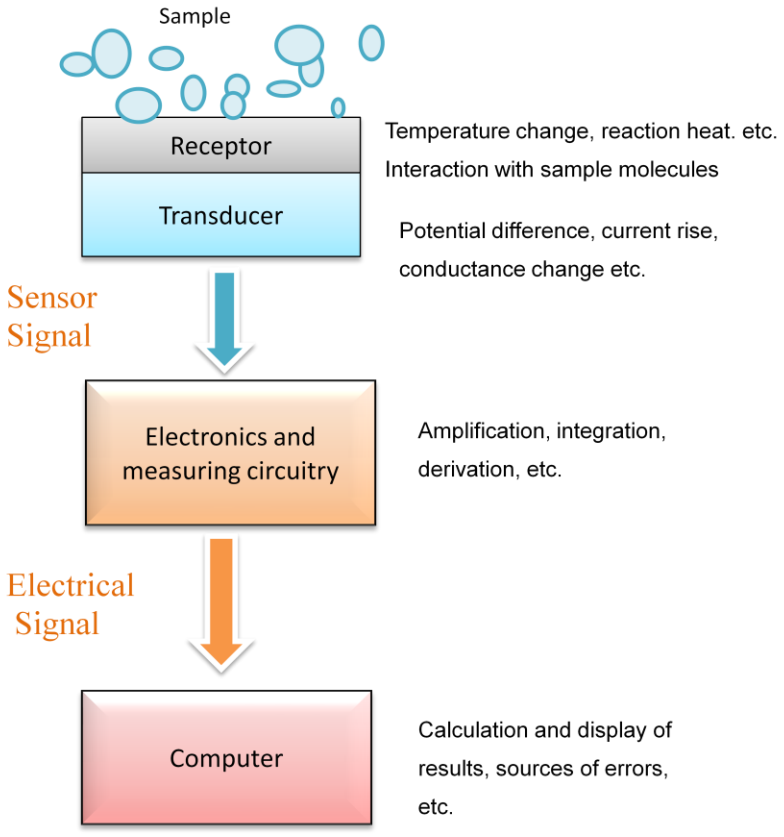

Figure 2-1 Scheme of a typical chemical sensor system

A chemical recognition (receptor) system, a physicochemical transducer, an electronics and measuring circuitry and a computer as shown in figure 2-1 are the general scheme that form a typical chemical sensor system [10]. In majority of the chemical sensors, the receptor interacts with the target analyte and as a result, its physical properties are changed in a way that the appending transducer gives a corresponding electrical signal. The receptor can be modified by the addition of any specific catalysts which would enable detection of specific chemicals. The transducer gives an output which corresponds to the specific reaction between the receptor and the target analyte. For example, a transducer may be a conductive material that changes its electrical conductance with reaction of the chemical and the surface. As another example, a transducer may modify the light passing through it depending on the presence of specific chemical. In order to process this data, some signal detection, amplification and processing are carried out to generate accurate information about the target chemical.

Sensors are frequently classified and named by their transduction method, e.g., conductometry; potentiometry; amperometry; gravimetry, which includes SAW (surface acoustic wave) and QMB (quartz crystal microbalance) transduction; optical (fiber optic, spectrometric, and refractometric); metal oxide semiconductor or MOX (heated metal oxide chemiresistive); conductive polymer chemiresistive; polymer composite chemiresistive; or capacitive. Alternately, they may be named according to their structure, as in MOS (metal-oxide-semiconductor) or MIS (metal insulator semiconductor) sensors. A third name is derived from the chemical reaction such as “sorption” sensors or “catalytic” sensors [13].

The challenge in the development of sensors is on designing, finding or fabricating new materials. The following discussion will focus on the chemical sensor

technologies which are broadly used. Generally speaking, the chemical sensors can be categorized as either resistive or capacitive. As the name suggests, a resistive sensor changes resistance (change in conductance) when exposed to a chemical of interest, whereas a capacitive sensor changes capacitance when exposed to a chemical of interest.

2.2 Electrochemical Sensors

Electrochemical sensors represent an important subclass of chemical sensors in which an electrode is used as the transduction element, and are highly qualified for meeting the size, cost, and power requirements of on-site environmental monitoring. Characteristics of electrochemical sensing systems include high sensitivity and selectivity, a wide linear range, minimal space and power requirements, and low-cost Instrumentation [14]. There are three basic electrochemical processes that are useful in transducers for sensor applications [15];

(i) Potentiometry

Potentiometry is the measurement of a cell potential at zero current. Electrochemical sensors based on potentiometry measure the open circuit (high imepedence) electrochemical cell potential, which according to the Nernst equation is proportional to the logarithm of the concentration of the chemical species of interest.

$$E = E^0 + \frac{RT}{nF} ln\left(\frac{C_O}{C_R}\right) \quad (1)$$

where E^0 is the standard potential of the electrode, R is the molar gas constant, T is temperature, F is Faraday's constant and C_o and C_R are the concentration of the oxidized and reduced forms of the species, respectively [16]. They are commonly used when the concentration of chemical specie to be measured changes over several orders of magnitude (e.g., in the case of pH measurements). In cases, where the concentration

changes over only one or two orders of magnitude, a sensor with a linear relationship between response and concentration is preferable (such as Amperometric sensors) rather than logarithmic response [17].

(ii) Voltammetry (Amperometry)

Voltammetry, in which an oxidizing (or reducing) potential is applied between the cell electrodes and the cell current is measured. The measured current is due to the response of chemical species of interest. Voltammetry improves the sensitivity by increasing the ratio of the faradaic current (the current of interest) and non-faradaic current. By applying linear, square or cyclic voltammetry, improved selectivity and sensitivity is achieved.

In cyclic voltammetry, a periodic triangular voltage waveform is applied between the working and the reference electrodes and the current response of the cell is monitored. The waveform is linearly scanned in a potential window with a lower or initial value of V_i and the upper or final value of V_f, at a given scan rate of v.The subsequent plot that is obtained is called cyclic voltammogram. Cyclic voltammetry is commonly used for microelectrode to reduce the non-faradaic current.

In chronoamperometry electrochemical analytical technique, the potential of the working electrode is stepped, and the resulting faradaic current (caused by the stepped potential) is measured as a function of time [16].

Amperometry is a special type of voltammetry, where the voltage applied across the electrodes of the electrochemical cell is kept constant while its current is measured. The measured current is a function of the concentration of the electroactive species. The response will have high linearity if the current is limited by the rate of the mass transfer and not by the rate of charge transfer [16].

(iii) Conductometry

In conductometry, the conductance of the (reciprocal of resistance) of the cell is measured by an alternating current bridge method. In this kind of sensor mostly the resistive component of the impedance of the chemical specie is measured. The conductance is related to current and potential through the generalized form of Ohm's law. If the measurement is done with AC signal conductance (G) becomes frequency-dependent conductance G(ω) and the resistance R becomes impedance Z(ω) [17].

2.3 Conductometric (Resistive) Chemical Sensors

The basic mechanism of resistive sensors can vary from sensor to sensor. The first principle behind the resistive sensor mechanism is either chemical reaction or polarization. Polarization can happen when either a small density of the DC current or small AC excitation amplitude is used or the selective layer has a high concentration of charge carriers. Also, a high concentration of carriers results in high conductance of the selective layer. Hence, the change in conductivity due to interactions with the analyte leads only to a very small relative signal change, $\Delta R/R_B$ [17].

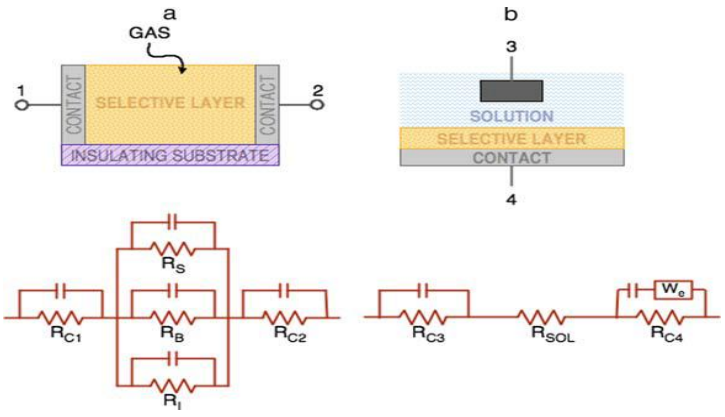

Figure 2-2 General chemiresistors and their equivalent circuits: (a) lateral configuration in which any of the five resistances can be modulated by chemical interaction; (b) impedimetric chemiresistor in which capacitance C_B is chemically modulated [17].

The sensitivity of resistive sensors can be parts per trillion (ppt) when they are activated or heated, though sensitivity may vary from sensor to sensor. The sensitivity of the conductometric gas sensors also depend on the value of the dissociation constant, on the solubility of the gas in the internal filling solution, and, to some extent, on the equivalent ionic conductance of the ions involved [17]. The statistical information on many sensors is not exactly available in most of the papers due to which an accurate performance characterization of sensors is not easy to conduct.

A drawback of general resistive sensors is that their base resistance is hard to control. Thus, consideration is given to the contact resistance (R_c) between the electrodes and the selective layer, the bulk resistance (R_b) and the surface resistance (R_s) of the selective layer, and the interface resistance (R_i) which is located at the interface between the selective layer and the insulating substrate [17]. For example, in the case of a carbon nanowire sensor, the resistance varies from 1 MΩ to 1 GΩ [18]. The resistance change is monitored when the sensors are exposed to NO_2 [19]. A fair comparison among the sensor is very difficult to conduct because of limited information provided by the published results.

Resistive chemical sensors are used because of their advantages: good sensitivity to relevant gases, low production costs, and small size. Thus, it is convenient to design miniature gas detection system with these sensors [20]. The response time of a resistive sensor is longer than that of capacitive sensor which can be considered as its disadvantage.

2.2.1 Carbon Nanotube (CNT) Chemical Sensor

Carbon nanotubes (CNTs) are one-dimensional nanomaterials, which have attracted great interest due to their unique special electrical, optical, mechanical and thermal properties and the large variety of potential electronic applications including gas

sensing [21]. The material properties involve interesting advantages for sensors, such as a short reaction time, a higher sensitivity and novel sensing principles [22]. Carbon nanotubes (CNTs) are graphene sheets rolled over into cylinders with diameters in the order of one nanometer. CNTs have nanometer range diameters and all the atoms exposed on the surface. This allows miniaturization and means for chemical coating to achieve high selectivity to specific chemical agents [19]. The important properties of CNTs are the higher sensitivity, the faster reaction time and the modulation of CNT behavior in contact with specific material. The properties of CNTs are modulated by interaction with atoms, ions or molecules. In fact the conductivity of a single CNT or a CNT film can be changed by changing the concentration of O, NO, CO and of alcohol vapor in its proximity. CNTs are either semiconducting or metallic. The band gap of the semiconducting CNTs is dependent on their diameters [22].

The above mentioned features of carbon nanotubes (CNTs) have generated interest in developing CNT-based sensors for many applications [23]. So many research and results were published on CNT sensors based on a bare CNT, a CNT transistor, and a film of CNTs [24]. The application of these sensors in next-generation sensors will revolutionizing the sensor industry due to their inherent properties such as small size, higher integration with the circuits, high strength, high electrical and thermal conductivity. As mentioned earlier, each type of CNT sensors has its own advantages, such high selectivity, high sensitivity, easier fabrication steps, and high yield.

Single-wall carbon nanotube (SWNT) sensors are popular CNT sensor. High surface-to-volume ratio, nanosized structure, and interesting electronic property enable SWNTs for its usage for sensor fabrication [9]. Single SWNTs are nanometer-diameter cylinders consisting of a single graphene sheet wrapped up to form a tube [25]. As discussed earlier about CNTs, SWNT can be either metals or semiconductors, and their

electrical properties can rival, or even exceed, the best metals or semiconductors known. The unusual electronic structure of the two-dimensional material, graphene, from which they are constructed, is the highlight for remarkable electrical properties of SWNTs.

SWNT - based sensors have been used for the detection of small gas molecules [26]. SWNT sensor in transistor configuration yields a detection level on the order of ppm at room temperature. It requires a temperature of >350°C for conventional metal oxide microfilm sensors. The room-temperature sensitivity of the SWNT sensors, which are fabricated like chemical field effect transistors, is attributed to drastic changes in the electrical conductivity of semiconducting SWNT induced through the charge transfer of gas molecules. Whereas, it is difficult to obtain semiconducting SWNTs from as-grown samples, which are typically mixtures of both metallic and semiconducting SWNTs. Even when nanotubes are directly grown on the platform by chemical vapor deposition, there is no control over the growth of semiconducting or metallic tubes' selectivity. This often results in fabrication complexity, low sensor yield, and poorly reproducible sensor performance [26]. Lack of selectivity is a major limitation for SWNT-based sensors. However, surface modification of SWNTs with a suitable molecular recognition system can enhance the sensitivity [9], i.e., multiple SWNT transistor arrays coated with a polymer film is used. It has improved sensitivity and selectivity at zero gate voltage. Next section discusses about a SWNT chemiresistive sensor arrays with surface modification to improve sensitivity.

2.4 Porphyrin – Functionalized SWNT Chemiresistive Sensor Arrays

The property of conductance change in SWNTs on absorption of an analyte gas molecule makes them a potential material for sensor development. Further, SWNTs, one-dimensional structures with a nanometer range diameter, make it possible to develop a high-density nanosensor array within a limited space. Porphyrins have been widely

investigated as functional materials for chemical sensor fabrication due to their several unique and interesting physicochemical properties [9]. Due to large stability and catalytic behavior several metalloporphyrins have found various applications in chemical analysis [27]. The rich chemistry of porphyrins, especially metalloporphyrins, results in a large variety of interaction mechanisms that can be utilized for chemical sensing [28].

The role of the coordination in a metalloporphyrin is considered of primary importance to determine the sensitivity and selectivity properties by axial binding of the analyte molecule. However, hydrogen bonding, polarization and polar interactions, may simultaneously be present and cooperate in the total guest molecule binding. Due to this extensive richness of interactions, metalloporphyrins have been widely used for the detection of toxic gases, environment pollutant nitro-aromatic compounds insecticides and pesticides [28].

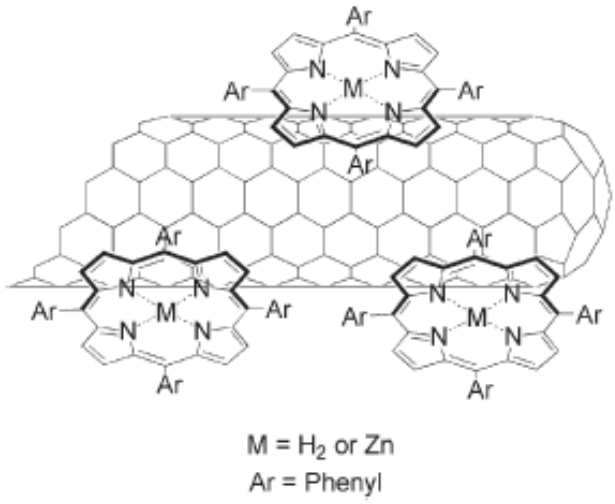

Figure 2-3 Representation of SWNT/porphyrin nanohybrids.

Porphyrin thin-film-based field-effect transistor (FET) has been reported as gas sensors, but its low conductivity is a prominent drawback. However, the SWNT−porphyrin hybrid, which can be prepared by surface modification of SWNTs with porphyrin, could

overcome the conductivity issue. In the SWNT−porphyrin hybrid, the high electrical mobility of SWNTs improves the device conductance, whereas the binding ability of porphyrin toward different analytes improves the sensing performance of the hybrid device when used as a sensory layer [9]. Figure 2-3 shows a structural representation of SWNT/Porphyrin nanohybrid [29].

The richness of the porphyrin library facilitates the independent development of SWNT−porphyrin hybrid based sensor arrays. To sense a wide spectrum of VOCs a nanosensor array based on porphyrin-functionalized SWNT hybrids operating in chemiresistive mode is introduced. Sensor arrays are micro fabricated on a highly doped p-type silicon substrate by standard lithographic patterning. Figure 2-4 shows a histogram comparing the responses of bare and free-base and metal-substituted porphyrin functionalized devices toward acetone, methanol, ethanol, MEK, and water (@100 saturated vapors) [9].

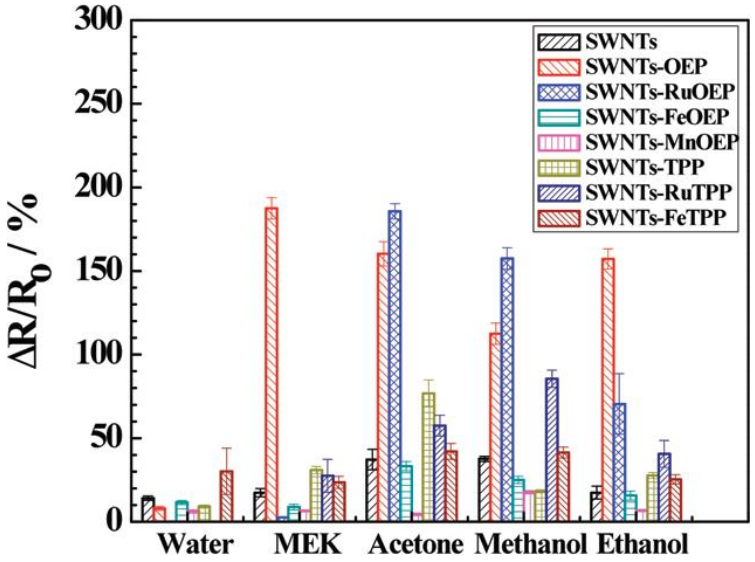

Figure 2-4 Histogram showing comparison of responses of bare and free-base and metal-substituted porphyrin functionalized devices

Figure 2-4 above shows the change in base resistance for the chemiresistive sensor arrays is less than 200 % and figure 2-5 shows the transfer characteristic of the one of the surface modified SWNT devices in the presence of air and saturated vapors of acetone which is one of the VOCs [9].

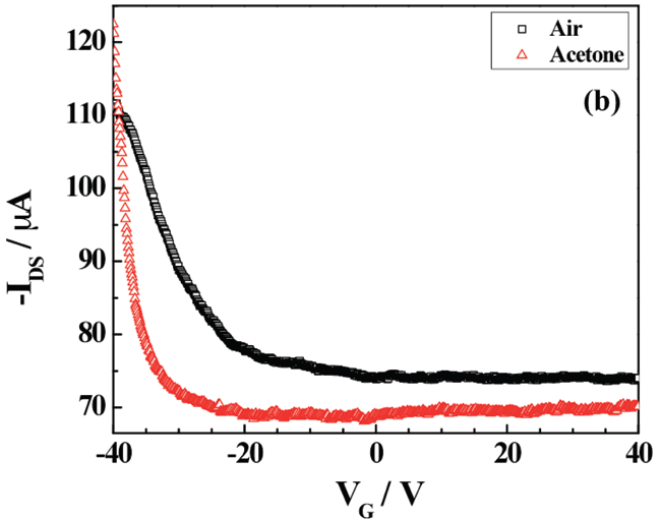

Figure 2-5 Transfer characteristic of surface modified SWNT sensor

Figure 2-6 Porphyrin-Functionalized Single-Walled Carbon Nanotube Chemiresistive Sensor Arrays for VOCs layout.

Figure 2-6 is the layout for the Porphyrin-Functionalized Single-Walled Carbon Nanotube Chemiresistive Sensor Arrays for VOCs [9]. This sensor has sixteen arrays of surface modified SWNT chemiresistive sensor arrays for the detection of different VOCs. So this sensor can be used to detect the toxic substances in the environment. These sensor arrays can differentiate analytes from one another because of the different hybrid materials used for the surface modification. This discriminating power of the hybrid devices and availability of the wide range of commercially available synthetic porphyrins open up an opportunity to develop a highly dense nanosensor array for E-nose applications [9].

2.5 Review of Conductometric Readout Circuits

Trans-impedance amplifier with a gain resistive feedback is the most widely used method for current measurement by converting input current I_{IN} to output voltage $V_O = -I_{IN}R_F$, where R_F is the transimpedance amplifier feedback or gain resistance. The schematic for the basic trans-impedance amplifier is shown in figure 2-7 below.

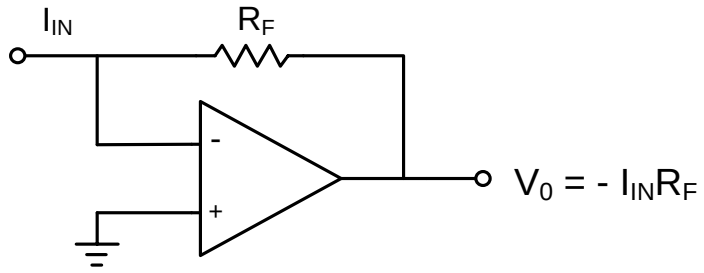

Figure 2-7 Current measurement using a trans-impedance amplifier.

The high gain operational amplifier (op-amp) forces a virtual ground at the working or counter electrode to allow the cell current to flow through the op-amp via feed-back resistance R_F, hence it generates an output voltage which is linearly proportional to I_{IN}. The I_{IN} for a conductometric sensor would be linear to a change in conductance when

the constant voltage is supplied at one end of the conductometric sensor. This method has a few drawbacks.

- The feedback resistor along with the capacitance of input device creates a pole at the input, degrading the stability and pulse response [30].
- Large value of feedback resistance is required to measure smaller input currents and very large resistors are difficult to realize in integrated circuit design [31].
- The feedback resistance generates thermal noise $4kTR_F$ where k is Boltzmann constant 1.38 x 10-23 J/K and T is 290K). This is an additional component in the output noise of trans-impedance amplifier [32].

Another approach is to use switch capacitor circuits like the one in Figure 2-8. When the clock signal is low, sensor current charges an integration capacitor to the output voltage. When the clock signal goes high, the capacitor is discharged. The circuit functions similar to trans-impedance amplifier with a feedback resistor. The gain of the switched capacitor circuit amplifier is controlled by the pulse width of the switch timing signal.

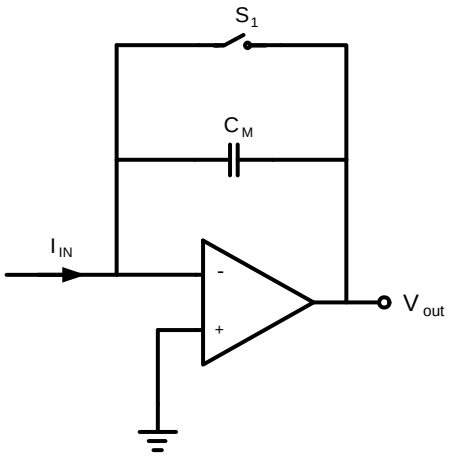

Figure 2-8 Switched capacitor trans-impedance amplifier

The switched capacitor trans-impedance amplifier does not have the thermal noise contributed by the feedback resistance in conventional trans-impedance amplifiers. The disadvantage is that it includes the switching noise caused by the switch which can leak and add to capacitor voltage. Another problem is that switched capacitor circuits are more complex than the simple one and involve several switches with different clock phases [33][34]. This requires good phase locking between the various clocks used for switching which extends the complexity of the system. This also adds a lot of substrate noise from digital switching which could affect the linearity of the output.

A third method for the conductance measurement is to place the sensor resistor in place of the feedback resistor in an inverting amplifier as shown in figure 2-9 [35].

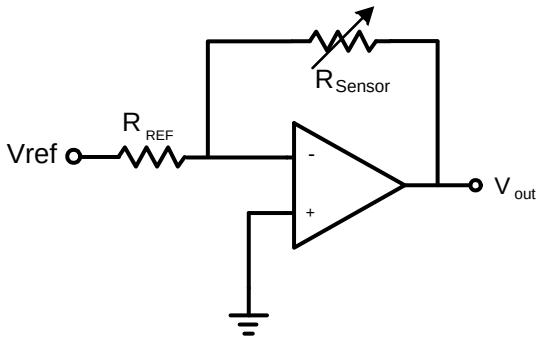

Figure 2-9 Inverting amplifier with conductometric sensor as feedback resistor.

For the configuration in figure 2-9 due to the very large open loop gain and high input resistance, the closed-loop gain of the inverting amplifier depends only on R_{ref}, and the sensor's resistance. The output of the amplifier thus reflects the conductance of the selected sensor element. The resistance of the pass-switches is known, and the output can be calibrated to compensate for this added resistance. Uncertainties in V_{ref}, R_{ref} and amplifier offset and gain will remain constant for all sensing elements [35].

Chapter 3

CMOS Conductometric Circuit for Chemical Sensing Using Nanowire Sensor Arrays

The conductometric circuit for the nanowire sensor array offers a small, portable prototype platform for chemical gas sensors to enable low power and continuous gas monitoring. This enables the detection of different types of VOCs present in the environment and can be used in electronic nose (E nose) applications. The circuit can read data from sixteen different sensors, and can be processed for the proper detection of the VOCs present. This chapter explains the design and analysis of the circuit. This is followed by a PCB implementation of the proposed circuit. Then the design analysis of the core circuits and the overall system in CMOS is discussed. The simulation and measurement results of the IC are shown at the end of the chapter.

3.1 Design of Conductometric Circuit for Nanowire Sensor Array

In electrochemical sensor system, the method of extracting the electric signal from the sensor has a great impact in the performance of the detection of the chemicals present. In a typical electrochemical system it is required to detect the signal properly in order to interpret the analyte concentration. Also one of the important requirements for measuring the VOCs is real time monitoring, i.e. the system should be portable and able to transfer the data obtained from the sensor with a portable device (Laptop, tablet or a smart phone).

This work proposes a conductomteric circuit based on the trans-impedance amplifier to readout the values from sixteen different sensor arrays to detect different VOCs present in the environment as shown in Figure 3-1. A VOC sensing system based on the change in the conductance of the chemiresistive sensor arrays requires high linearity and low power. This gives it a wide input dynamic range to measure a wide range of concentrations of VOCs present in the environment.

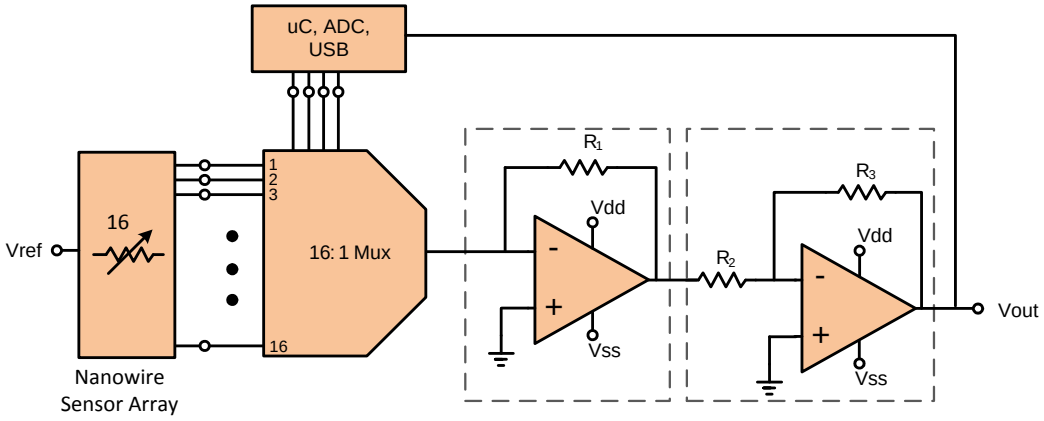

Figure 3-1 Proposed conductometric circuit for the nanowire sensor array

Figure 3-1 shows a 16:1 analog multiplexer and current to voltage (I-V) converter circuit. The I-V part of the circuit is common to all TIA amplifier systems and is implemented using op-amp with a feedback gain resistor. The I-V converter is followed by an inverting amplifier (buffer) which inverts the output of the TIA to read the signal with an analog to digital converter present in the microcontroller. The functional description of each block is explained below.

The sensor has sixteen chemiresistive arrays in which one end of each sensor connected with a common reference voltage as shown in Figure 3-1. The other ends of the arrays are connected to a 16:1 analog multiplexer. The analog multiplexer is used to select one chemiresistive sensor array at a time, which would enable the detection of the concentration of a particular chemical. The selection of the sensor array is done using the four select lines of the multiplexer. These four select lines are controlled by a microcontroller which is programmed to select respective sensor arrays. While designing the analog multiplexer the signal loss has to be minimized. Since the current path through the analog multiplexer offers a resistance which would cause a change in the actual value. This brings in the requirement of very low on resistance for the analog multiplexer.

Depending on the presence of the VOCs, the conductance of the chemiresistive sensor array varies and a corresponding change in current is also observed. Once a sensor array has been selected, the current starts to flows through the analog multiplexer which will be entered into the TIA stage. This TIA stage converts the input current into voltage according to the gain resistor value. The output voltage of the TIA is given by (2),

$$V_{out1} = -I_{in} * R_1 \quad (2)$$

This V_{out} is then inverted to make it a positive value by the following inverting stage buffer and the voltage is fed into the internal ADC of the microcontroller. Then the final output for the circuit is given by (3).

$$V_{out} = (-I_{in} * R_1) * (-\frac{R3}{R2}) \quad (3)$$

When R3 = R2, the value of the output voltage is same as the value of TIA output. The microcontroller processes this voltage value through its internal ADC and can send the data to a PC, tablet or smart phone for further processing.

For noise analysis of the proposed system in Figure 3-1 is simplified to the system in Figure 3-2. The conductometric sensor model is reduced to a parallel RC circuit of R_1 and C_1. The first stage of any system is the dominant noise source. The gain of the I-V converter reduces the relative noise contributed by the inverting amplifier.

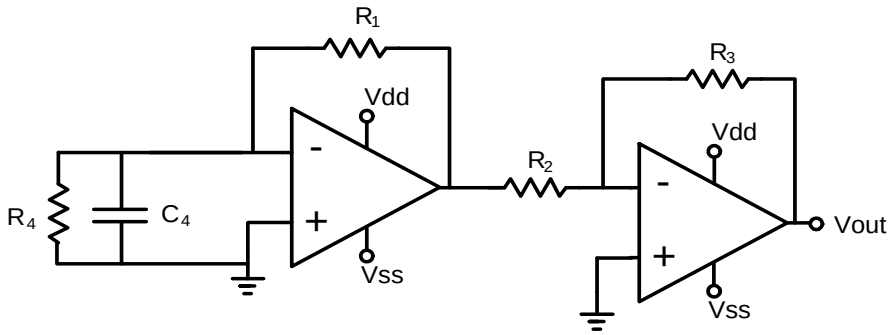

Figure 3-2 Conductometric circuit with reduced sensor model for noise analysis

Equation (4) gives the noise gain of I-V converter using reduced sensor model

$$A_{noise} = 1 + \frac{R_1}{R_4}(sR_4C_4 + 1) \tag{4}$$

Op-amp noise includes thermal and flicker noise generated by the FET transistors. At low frequencies the flicker noise is more significant than thermal noise.

$$\begin{aligned} V_{n_{opamp1}}^2 &= V_{n_{th}}^2 + V_{n_f}^2 = 4kTR_{opamp}B + K_{opamp}\sqrt{\left(\ln\frac{f_c}{f_1}\right)} \\ &\approx K_{opamp}\sqrt{\left(\ln\frac{f_c}{f_1}\right)} \end{aligned} \tag{5}$$

Noise gain of the system now includes the gain of the inverting buffer

$$V_{n_{total}}^2 \approx V_{n_{opamp1}}^2 \bullet A_{noise}^2 = V_{n_{opamp1}}^2 \bullet \left(A_{I-V} \bullet A_{INV}\right)^2 \tag{6}$$

Inserting the gain equation of I-V converter analyzed earlier and the integrator gain equation analyzed from the figure above, we get:

$$\begin{aligned} V_{n_{total}}^2 &\approx V_{n_{opamp1}}^2 \bullet A_{noise}^2 \\ &= K_{opamp}\sqrt{\left(\ln\frac{f_c}{f_1}\right)} \bullet \left(\left(1+\frac{R_2}{R_1}\left(sR_1C_1+1\right)\right)(1)\left(\frac{R_4}{R_3}\left(\frac{1}{sR_4C_4+1}\right)\right)\right)^2 \end{aligned} \tag{7}$$

3.2 PCB Implementation

Before implementing the conductometric circuit in CMOS technology, a Printed Circuit Board (PCB) prototype of the system is developed on a FR4 board. The components used are surface mount device (SMD) and through hole type for this implementation. The LTC2050 from Linear technologies was chosen for the op-amp since it had a high gain and low offset with a dual power supply. The analog multiplexer chip from Maxim Integrated was one of the ICs which provide very low on resistance. The PIC24 series microcontroller from Microchip has a 10 bit internal analog to digital (A/D)

converter and an integrated on-the-go USB module as well. This helped the PCB prototype to be powered directly from the PC, which helped us to do a real time monitoring without the need of carrying an external power supply module. The design of the PCB prototype is explained in the below section.

3.2.1 PCB Design

The PCB protoype built in this work is for a 16-array chemiresistive sensor and it can detect the sensor resistance variations between 10K to 100KΩ range. A dc voltage V_{ref} is applied across the sensor and its corresponding dc current is measured. This measured current is converted into voltage by using a trans-impedence amplifier based on op-amp and this voltage value is given to the internal ADC of the PIC microcontroller. The PIC microcontroller can read the ADC value and can communicate with the host using on-the-go USB protocol.

The schematics and layout for the system is done using the COTS components. Figure 3-3 and figure 3-4 shows the schematics for the conductometric circuit PCB prototype for the chemiresistive sensor arrays respectively. Figure 3-3 shows the power supply, voltage converters, USB connector and the programmer/debugger connections for the entire system PCB prototype to be functional. The power supply and voltage converters provide the necessary voltage levels to the all the COTS components used in the design. The programmer/debugger connector enables the PCB to be programmed in order to read the corresponding values from the sensor array, process the ADC values and communicate with the host via USB as well.

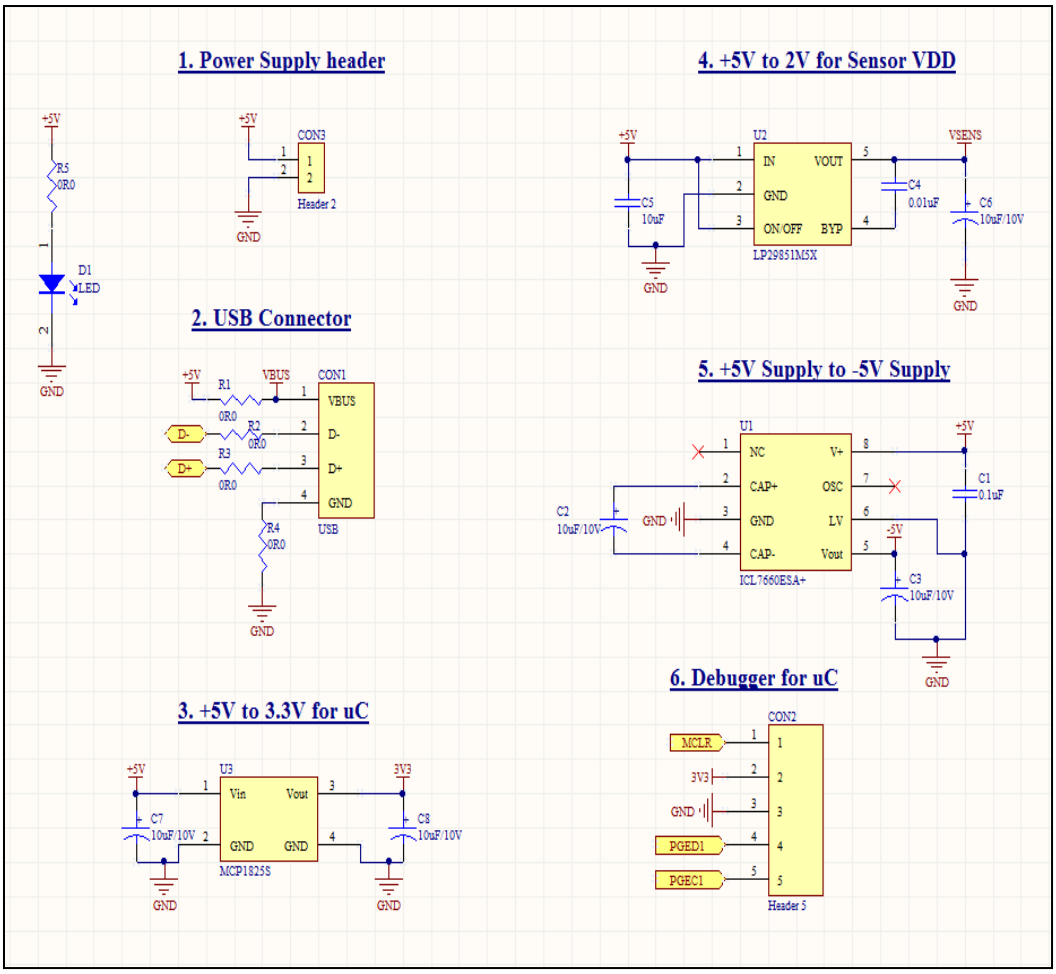

Figure 3-3 PCB schematics – Power supplies and Connectors

Figure 3-4 shows the schematics for the chemiresistive sensor arrays package, 16:1 analog multiplexer, trans-impedence amplifier based on op-amp, inverting buffer, PIC24F series microcontroller and its related circuitry.

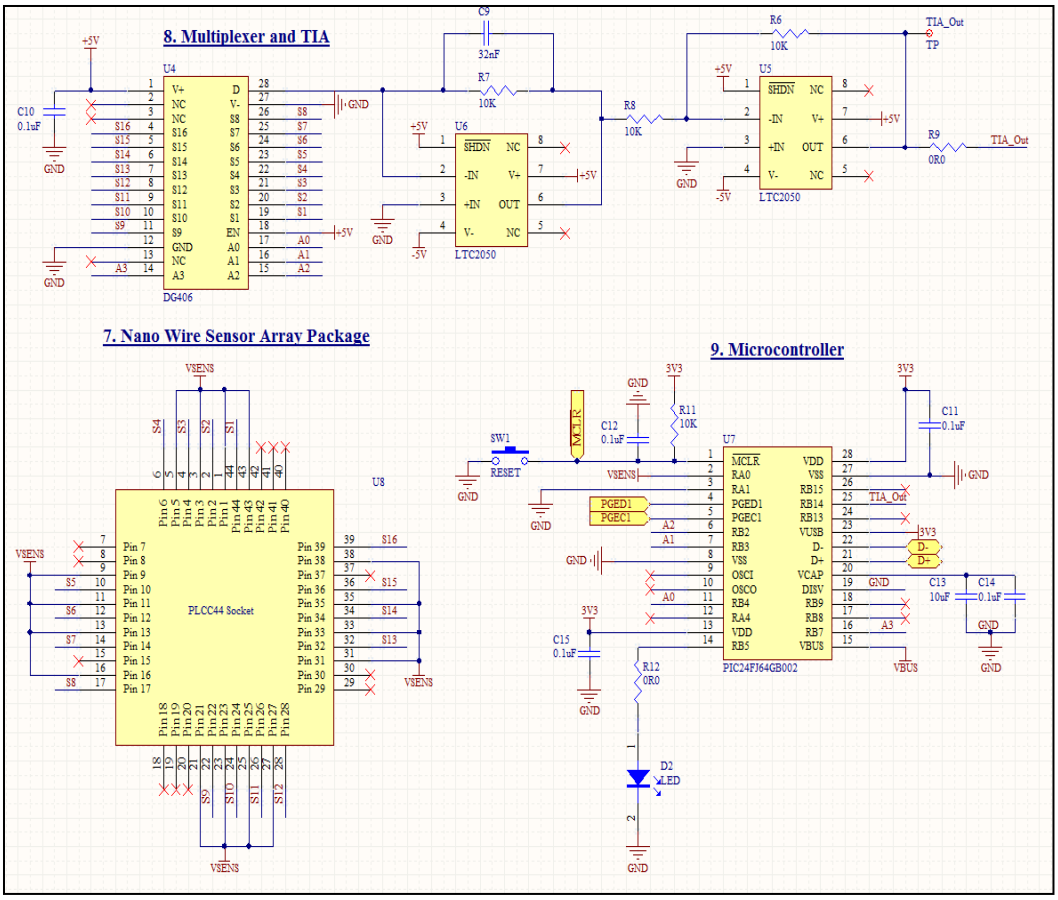

Figure 3-4 PCB schematics – TIA and control circuitry

The dimension of the PCB is 2.19 in X 1.98 in. Figure 3-5 shows the assembled PCB prototype for the conductometric circuit for chemiresistive sensor arrays which includes the USB connector and the PIC microcontroller.

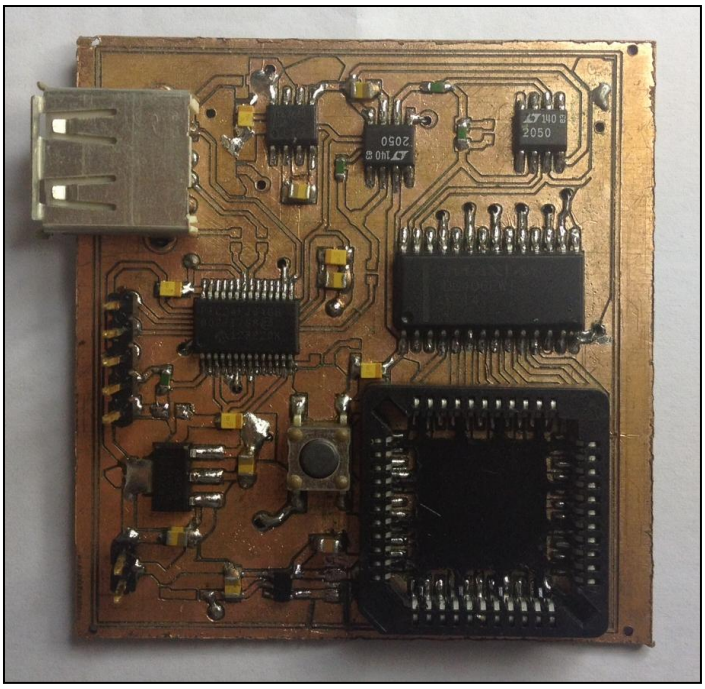

Figure 3-5 Assembled PCB Prototype

3.2.2 PCB Measurement Results

The measurement set up of the PCB prototype is shown in Figure 3-6.

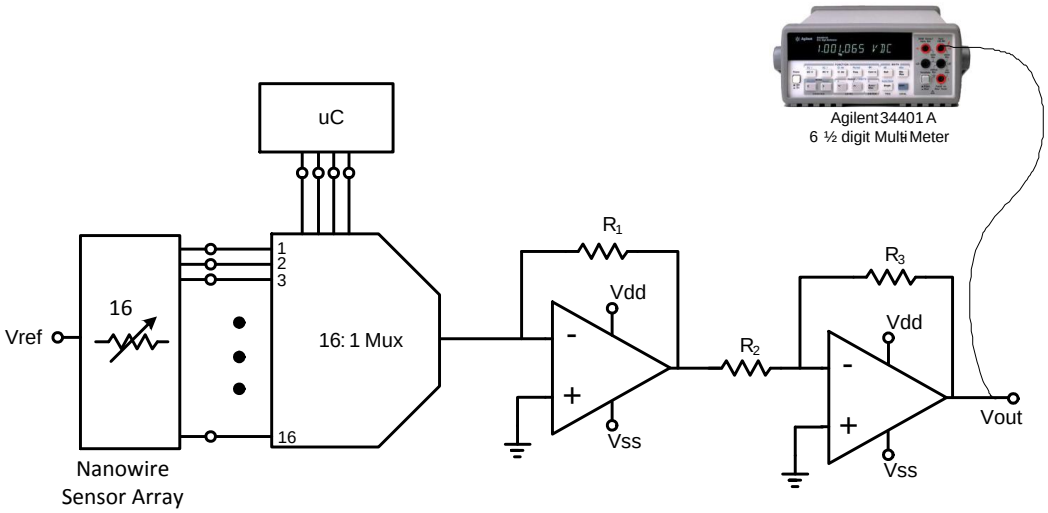

Figure 3-6 Measurement setup for the PCB prototype

The comparison of simulated and measured output voltage is shown in figure 3-7. The plot shows a fairly linear output.

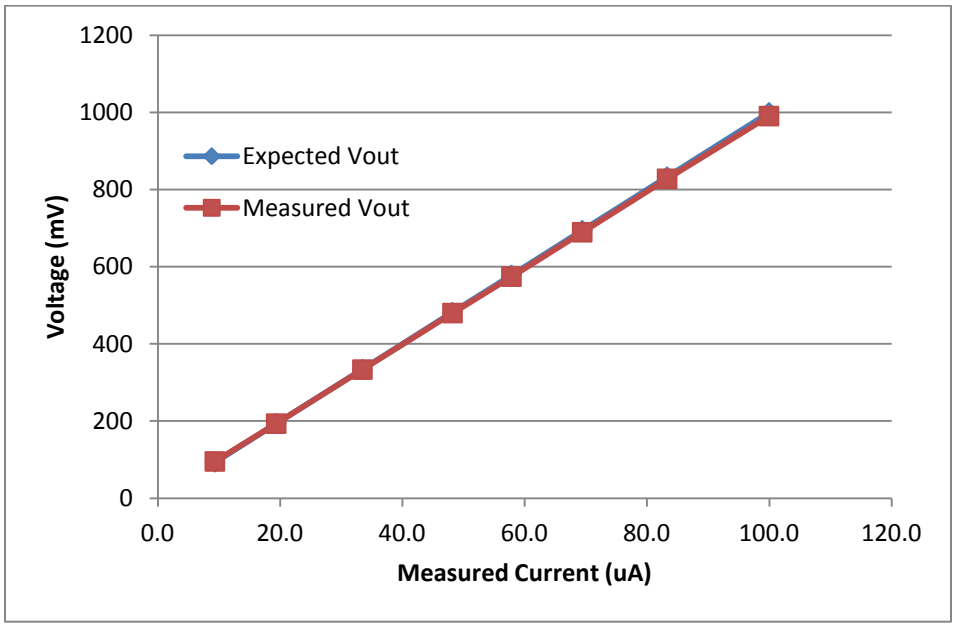

Figure 3-7 Comparison of measurement and simulated output

3.3 CMOS IC Implementation

The proposed CMOS conductometric circuit for chemical sensing using nanowire sensor arrays is designed and implemented in 0.35um CMOS process. This section includes the design and analysis of the op-amp and the analog multiplexer and the simulation and measurement results of the final integrated system.

3.3.1 Operational Amplifier

The op-amp should achieve good linearity over the input range of 1uA to 100uA current variation observed from the chemiresistive sensor array. The op-amp should also have high gain to reduce the gain error due to feedback. The telescope cascode op-amp provides very large gain due its cascode structure, but their output swings are relative limited due to overdrive voltages of the stacked transistors. Two stage op-amps provide relatively larger output swing while providing equally large gain as the telescopic op-

amps, but in order to reduce the gain error due to feedback a higher gain op-amp is required. For that reason, the architecture chosen which should provide a really high gain along with the maximum output swing in order to utilize the entire available voltage headroom. For this work, to achieve the primary goal of I-V conversion of the full output current range (because of the change in conductance) of the chemiresistive sensor array, a three stage op-amp is chosen. Figure 3-8 show the schematic of the three stage op-amp which is used in this work.

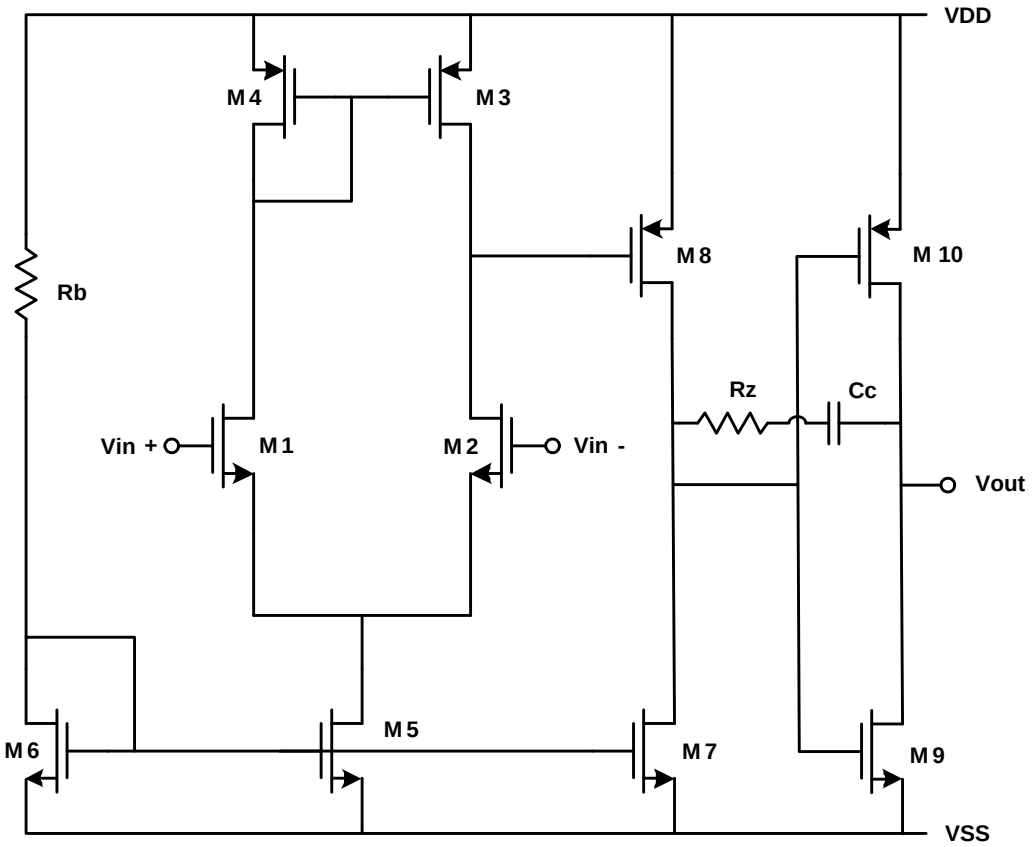

Figure 3-8 Three stage op-amp schematic

The op-amp is a differential-to-single ended type with NMOS input pairs. Due to their higher mobility the NMOS input pairs give higher gain and lower noise as compared

to PMOS input pairs. To increase the gain of the op-amp two additional common source amplifier stages are implemented which also improves the output swing. The dc gain of the op-amp is given by the multiplication of three stages, which is given in (8) and (9).

$$A_v = A_1 * A_2 * A_3 \tag{8}$$

$$A_v \approx \left(g_{m1} * \left(r_{o2} \| r_{o3}\right)\right) * \left(g_{m8} * \left(r_{o7} \| r_{o8}\right)\right) * \left(2g_{m1} * \left(r_{o9} \| r_{10}\right)\right) \tag{9}$$

Proper biasing of the transistors are critical to achieve maximum gain and voltage output swing. The biasing done using the resistor R_b along with the diode connected transistor M6. The channel length of this transistor increased in order to decrease the bias current change caused by process variations and channel length modulation. Transistor M5 acts as the tail current source for the differential pair. The channel length of transistor M5 is also increased in order to increase the common mode rejection ratio of the op-amp and also to reduce the effects due to process variations as well. The minimum output voltage of the op-amp is the overdrive voltage of the transistor M9, which is given by (10) below.

$$V_{out(\min)} = V_{ov} = \sqrt{\frac{2.I_{D9}}{\mu C_{ox} W_9 / L_9}} \tag{10}$$

The device dimensions (length) of MOS transistors in the op-amp circuit are chosen to maximize the overall gain and minimize the mismatch introduced due to process variation. The increased length of the transistors is also less prone to channel length modulation effect. The op-amp used in this work is used to drive capacitive loads and high impedance loads, which eliminates the requirement for an output buffer stage for the amplifier. The output resistance of the op-amp shown in figure 3-8 is given by equation (22).

$$R_{out} \approx 2 * \left(\frac{1}{g_{m10}} \| \frac{1}{g_{m9}}\right) \tag{11}$$

Op-amp noise analysis

Due to the demand for high sensitivity in the current readout circuit, care has been taken to minimize the noise power due to the amplifiers. In the noise analysis of these amplifiers, only devices in the signal path are important. Also, noise contribution of the tail current source transistors is cancelled by the differential symmetry and matching. The resulting input referred noise spectrum of the amplifier can be expressed as in (12).

$$\overline{\mathrm{v}_{\mathrm{n,tot}}^2} = 2\left[\overline{\mathrm{v}_{\mathrm{n1}}^2}(\mathrm{f}) + \left(\frac{\mathrm{g_{m4}}}{\mathrm{g_{m1}}}\right)^2 \overline{\mathrm{v}_{\mathrm{n2}}^2}(\mathrm{f})\right] \tag{12}$$

where $\overline{v_{ni}^2}(f)$ represents the noise spectral corresponding to the i^{th} transistor due to both thermal and 1/f component and g_{mi} is the transconductance of transistor M_i. Substituting the thermal noise and 1/f noise of M1 and M4 into the input voltage noise spectral yields,

$$\overline{v_{n,tot}^2} = \frac{16kT}{3\sqrt{2\mu_n C_{ox}\left(W/L\right)_1 I_{DS1}}}\left(1 + \sqrt{\frac{2\mu_p\left(W/L\right)_4}{\mu_n\left(W/L\right)_1}}\right) \tag{13}$$

$$+\frac{2k_{fn}}{C_{ox}(WL)_1}\frac{\Delta f}{f}\left[1 + \frac{2\mu_p k_{fp}}{\mu_n k_{fn}}\left(\frac{L_1}{L_3}\right)^2\right]$$

(13) shows that an increasing W/L for the input devices and increasing the tail current will decrease the thermal noise. Since μ_n > μ_p, the amplifier with NMOS inputs has less thermal noise than one with PMOS input devices [33].

Figure 3-9 shows the op-amp gain and phase plot. The op-amp achieves a 118.1 dB open loop dc gain and 59.73 degrees phase margin for a load capacitance of 100fF.

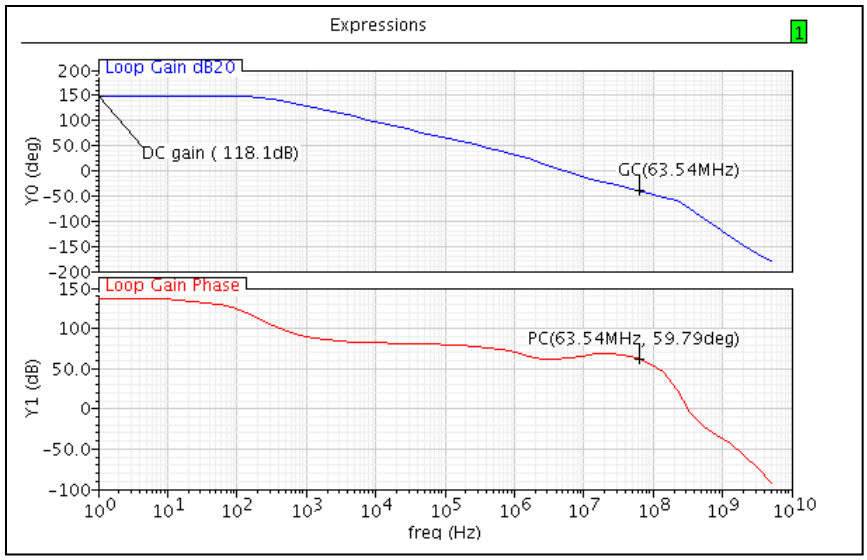

Figure 3-9 Op-amp Gain and Phase plot

To measure the output and input swing, the op-amp was simulated with unity-gain buffer configuration by shorting the output with the negative input. The positive input was swept with a DC Voltage from VDD to VSS. The output vs input curve is shown in Figure 3-10. The output swing of -1.55V to 1.6V is achieved.

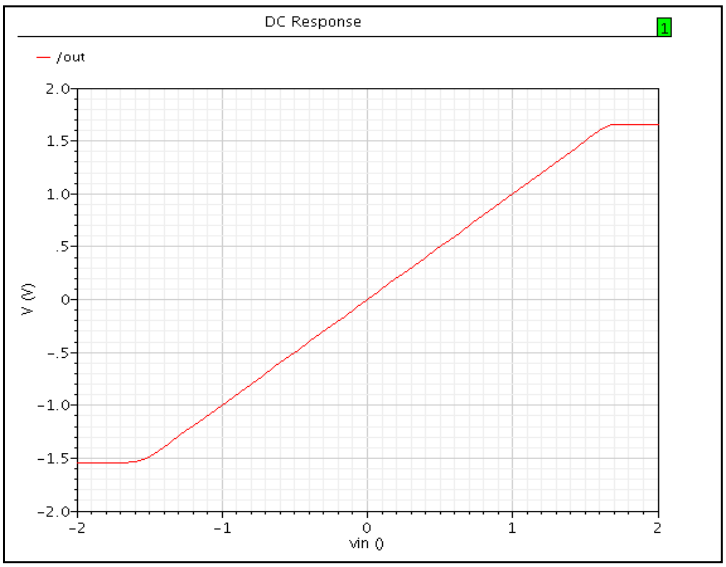

Figure 3-10 Op-amp DC response

The op-amp performance parameters from schematic simulation are summarized in the table below.

Table 1 Summary of op-amp performance parameters

Parameters	Value
Power Supply	±1.65V
Gain	118.1 dB
3dB Bandwidth	240 Hz
Unity Gain Bandwidth	63.54 MHz
Phase Margin	59.79 deg
Output Swing	3.15V

3.3.2 16:1 Analog Multiplexer

The analog multiplexer is the front end of the sensor array readout system, i.e. the sixteen chemiresistive sensor arrays will be connected to the 16:1 analog multiplexer of the readout system. This analog multiplexer then selects the corresponding sensor channels based on the microcontroller select outputs which can be controlled by the user.

The 16:1 Multiplexer consists of 16 switches and a 4:16 decoder. The schematic of the switch is shown in figure 3-11 below. There will be 16 similar switches in a 16:1 analog multiplexer which would be the inputs for the sensor outputs.

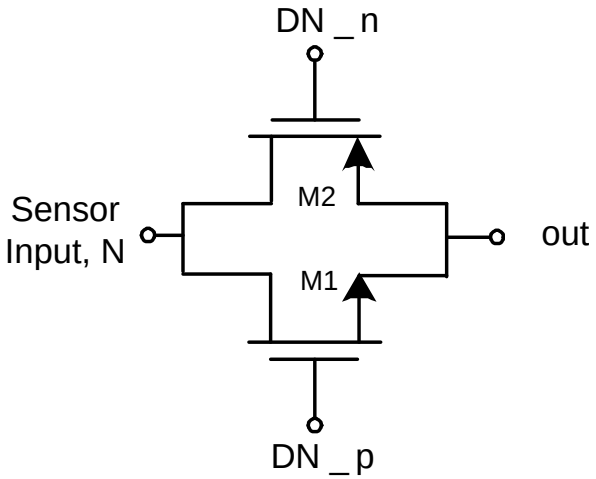

Figure 3-11 Transmission gate as switch for the multiplexer inputs

The switch as shown in figure 3-11 is realized using a transmission gate. A transmission gate is an NMOS and PMOS pair with their drains and sources connected. The gates are required to be connected to two differential signals DN_n and DN_p (where N represents the channel number). To achieve this, the outputs of 4:16 decoder circuit are also inverted so as to provide differential signals for the switch. To check the transient response of the transmission gate switch, a voltage source with a series resistance at the input to simulate a sensor and an ideal op-amp based TIA is at the output is given as shown in figure 3-13.

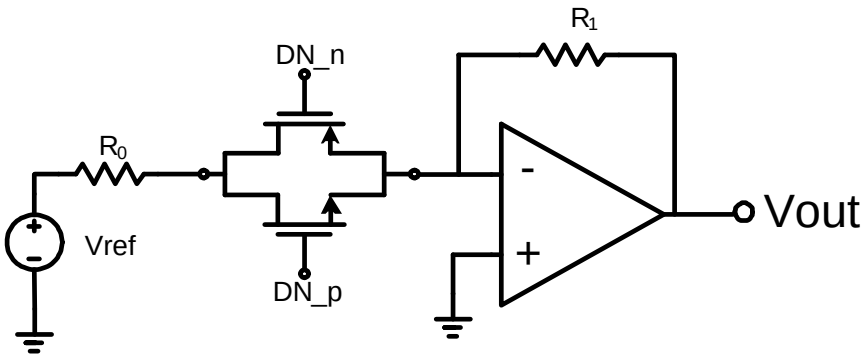

Figure 3-12 Transmission gate switch setup

The values given for V_{ref} = 1V and With R1 = 10kΩ. From transient response shown in figure 3-13, the simulated output voltage of the TIA for R0 of 10kΩ and 100kΩ is -994.1mV (ideal = -1V) and -99.94mV (ideal = -100mV) respectively. This drop is voltage is caused by the finite resistance of the switch. The channel width for the NMOS and PMOS are increased to reduce the on resistance of the switch. This helps to reduce the voltage drop across the switch when the current is passing through the switch.

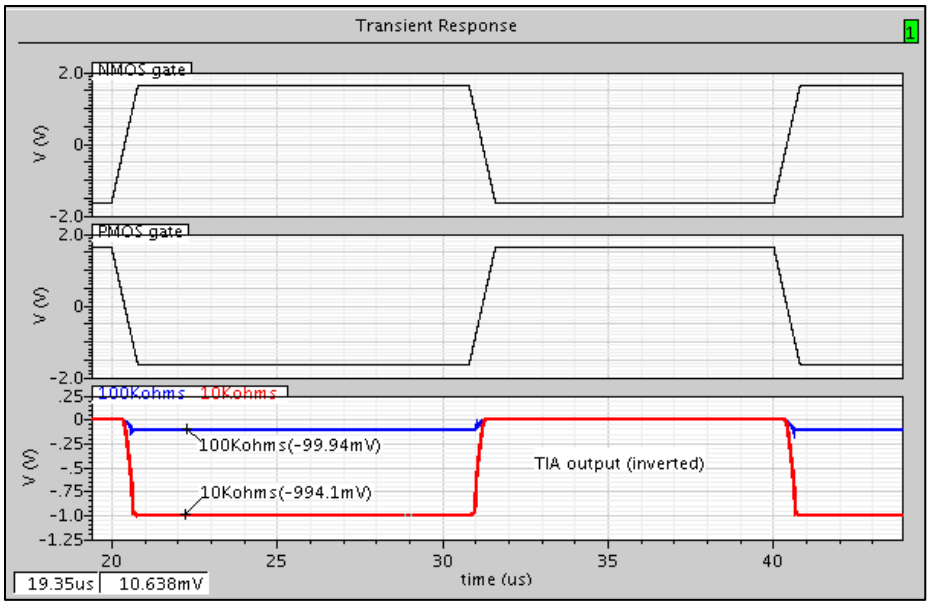

Figure 3-13 Transient response of transmission switch

In order to select the corresponding sensor array channel, corresponding transmission gate switches should be selected. The 4:16 decoder logic circuit enables this selection. The 4:16 decoder is a binary-coded decimal decoder which converts the 4 select pins S0 - S3 to 16 outputs D0 - D15 as shown in the figure 3-14 below.

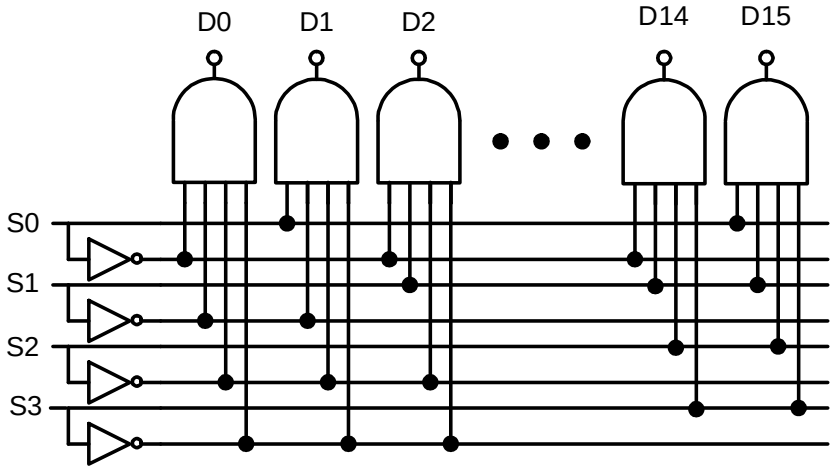

Figure 3-14 4:16 decoder logic

The decoder consists of CMOS logic NOT and NAND gates. The circuits of NOT, NAND and a single switch are shown in figure 3-15 below:

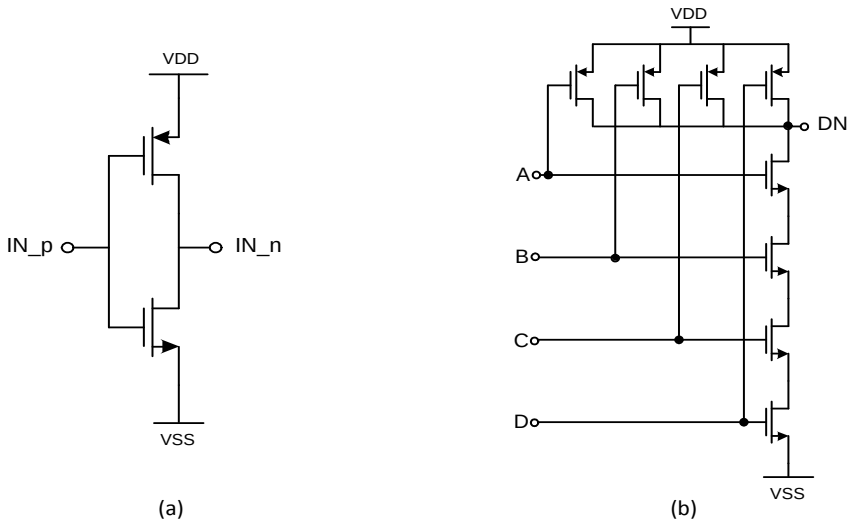

Figure 3-15 CMOS Logic gates. (a) NOT gate. (b) 4 input NAND gate

Transient response of the NAND gate is shown in figure 3-16. It is seen that for various combinations of the inputs A, B, C and D, a high on output (red) is obtained only when all four inputs are high. The inverted output (blue) is also shown in figure 3-16.

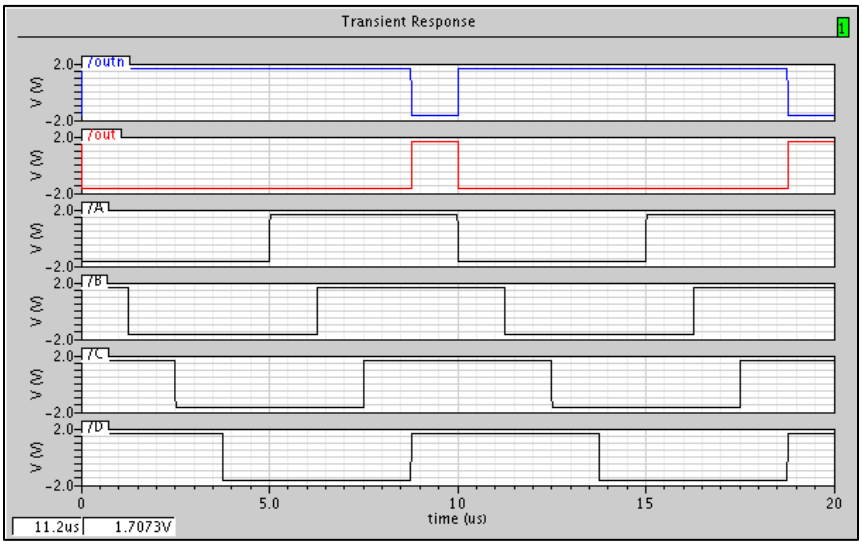

Figure 3-16 Transient response of NAND gate

3.3.3 Simulation Results

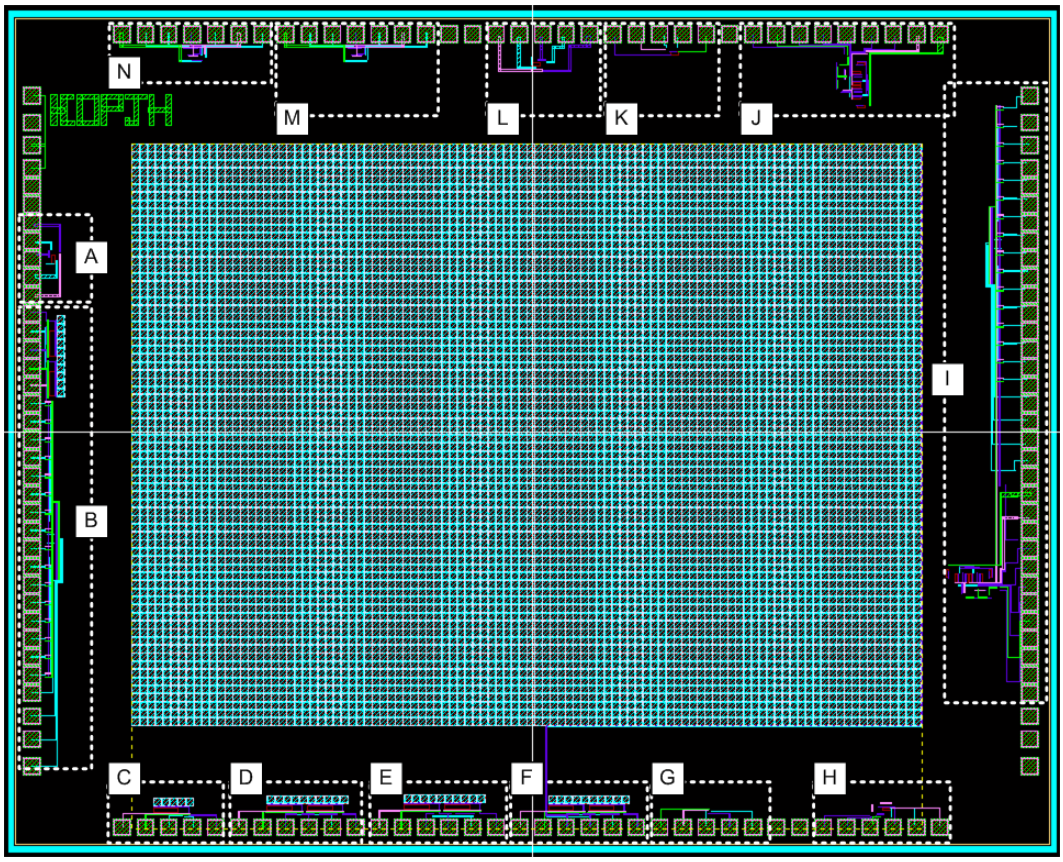

Figure 3-17 Complete chip layout screen shot.

The proposed circuit as shown in figure 3-17 is fabricated in 0.35um CMOS process. Cadence virtuoso tool was used for schematic design, layout design and routing. Assura was used for the DRC check, LVS check and RC extraction of the layout. The PAD size is 81.4um X 81.4um. The total area of the proposed conductometric readout circuit is 185um X 2300um.

The system DC response for input range of 10uA to 100uA is shown in Figure 3-19. The output range is from 101.7 mV to 1016 m V and is linear. This corresponds to a sensor resistance variation in the range between 10 KΩ to 100 KΩ with 1 V reference voltage given to one end of the sensor array.

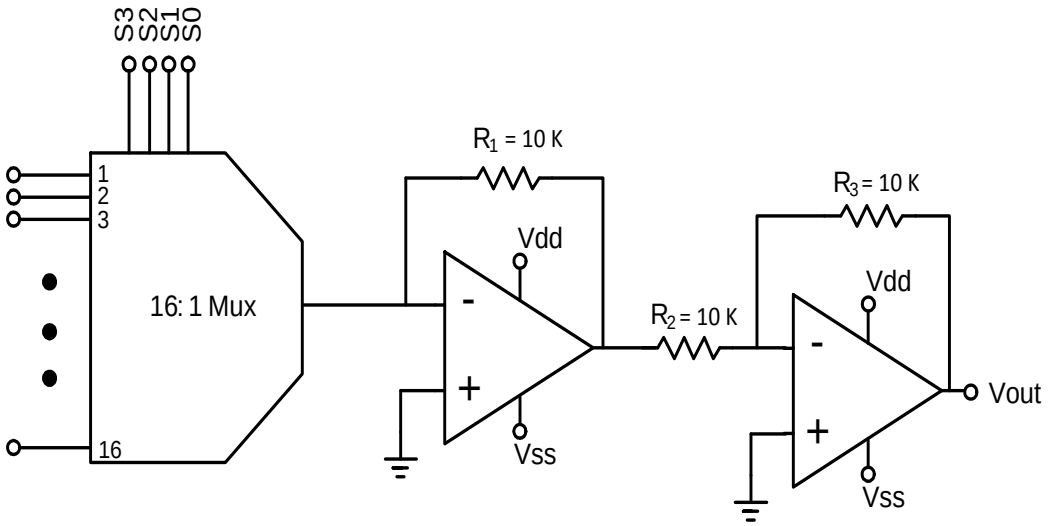

Figure 3-18 CMOS Conductometric readout circuit

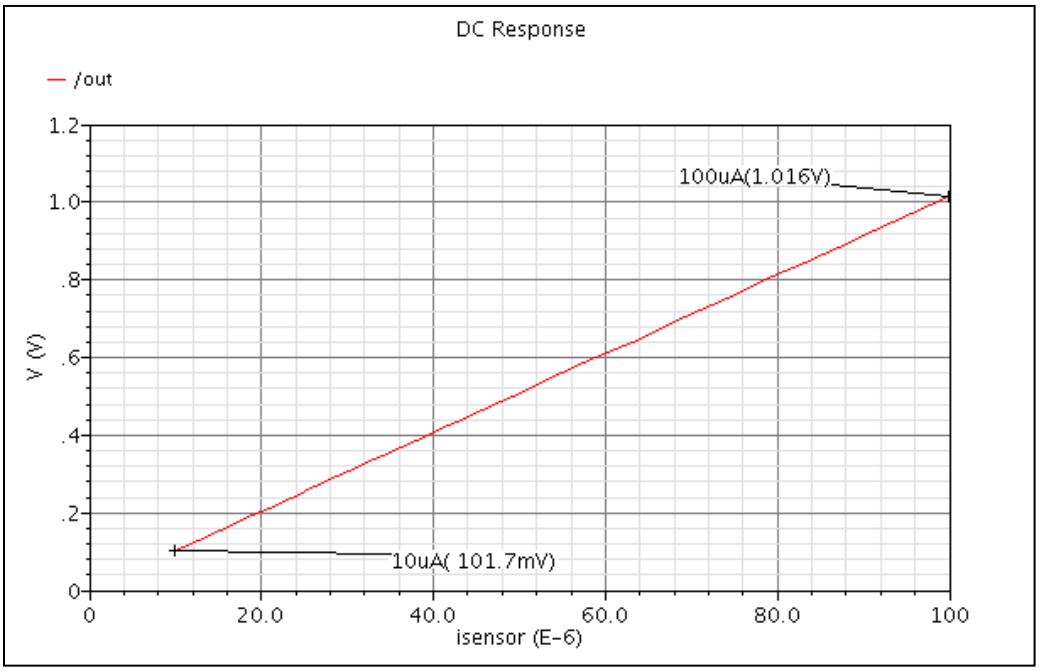

Figure 3-19 Conductometric readout circuit DC response

3.3.4 Measurement Results

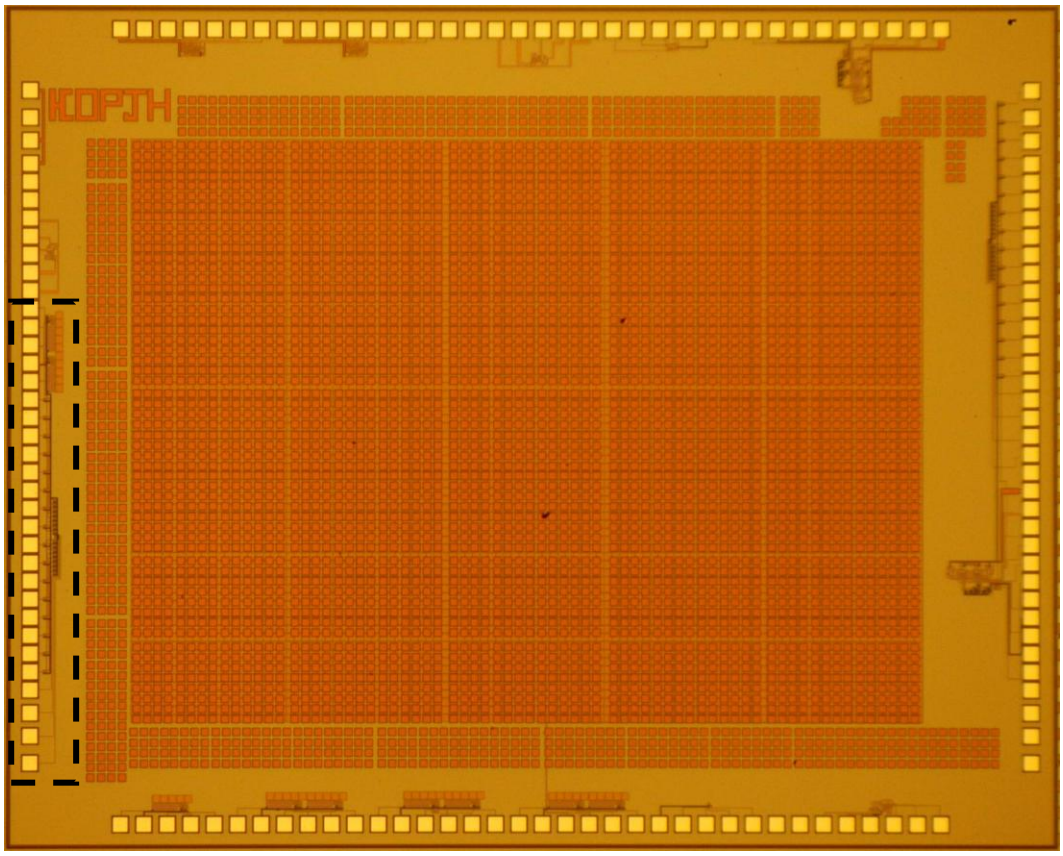

Figure 3-20 Fabricated chip photo

The packaged chip photo containing the conductometric circuit for nanowire sensor arrays fabricated in 0.35um CMOS process is shown in Figure 3-20 and the measurement setup is shown in Figure 3-21. The fabricated circuit is shown inside the black dashed box in figure 3-20. The package chip is tested using an adapter board. Keithley 2400 source-meters are used to provide constant voltage and a potentiometer is used to vary the resistance which in turn was changing the input current to the readout circuit. An Agilent 34401A multi-meter is used to read the output of the readout circuit.

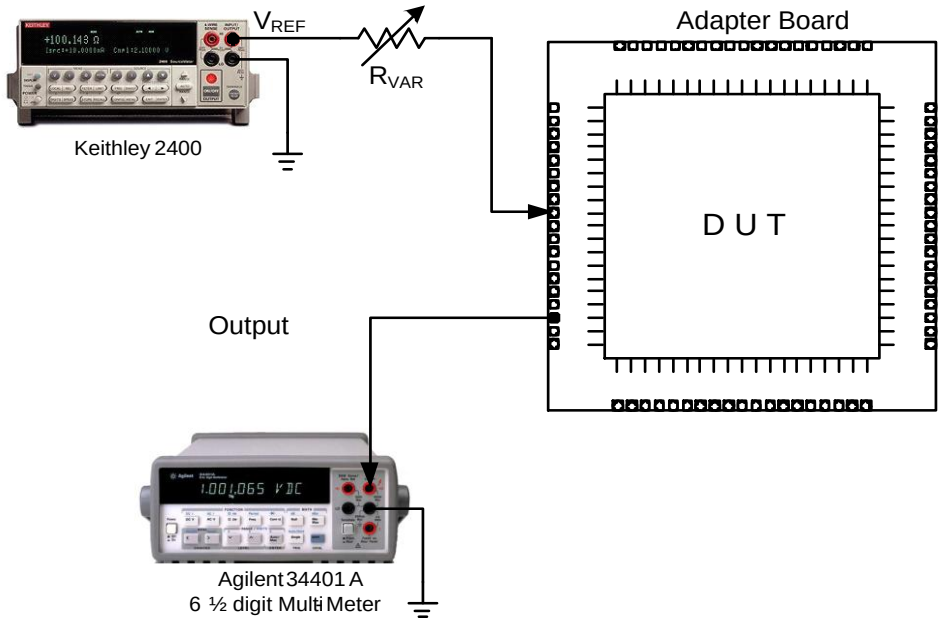

Figure 3-21 Measurement setup for DC response

Figure 3-22 shows the DC response of the conductometric system. The measurement result shows a good match with the simulation result. The measured result plot and simulated plot is shown in Table 2.

Table 2 Output vs. Input measurement readings for conductometric circuit

Resistance (KΩ)	**Input Sensor Current (uA)**	**Simulated Output Voltage (mV)**	**Measured Output Voltage (mV)**
10.00	100.0	1008	1081
12.00	83.3	843	892
14.40	69.4	703	745
17.28	57.9	586	626
20.74	48.2	488	515
29.86	33.5	339	367
51.60	19.4	196	198
106.99	9.3	95	88

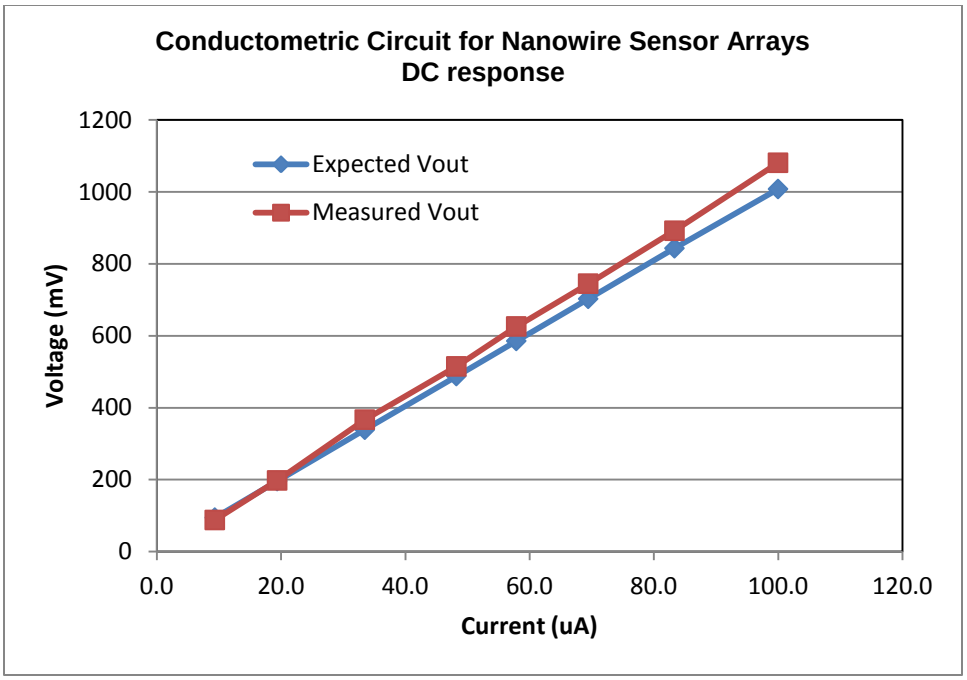

Figure 3-22 Output vs. Input measurement for conductometric circuit.

Table 3 summarizes the measurement results of the proposed analog correlator based readout circuit.

Table 3 Summary of measurement results

Parameters	Measurement result
Range	10KΩ to 106KΩ
Gain	10.54KΩ
Power	6.07 mW

Chapter 4

Conclusion

In this work, a conductometric circuit for chemical detection using nanowire sensor arrays based on conductometric electrochemical sensing is proposed. It is designed to work with the output range of a novel Porphyrin-Functionalized Single-Walled Carbon Nanotube Chemiresistive Sensor Arrays for VOCs. This single-walled carbon nanotube−porphyrin hybrid based chemiresistive nanosensor arrays is designed for monitoring toxic substances in the environment. The conductometric based readout circuit can achieve the required resistance variation range (10KΩ to 100KΩ) from the chemiresistive sensor arrays and show a linear output in that range. The conductometric based readout circuit offers portability and real time monitoring of toxic substances in the environment with the help of a smart phone, PC or a tablet and is a better solution for the readout circuit for the sixteen arrays of chemiresistive sensor. This circuit is implemented in two different ways: first a PCB implementation and then a CMOS integrated circuit implementation.

In the PCB implementation, the circuit is designed using COTS components on an FR4 board. It is tested with conductometric (resistive) electrochemical sensor model implemented in passive components. The measurement results show that the COTS system of functions in the sensor resistance range of 10KΩ to 100KΩ giving a linear output range of 1.00V to 0.1V. Hence the PCB implementation can be successfully interfaced with a sixteen channel Porphyrin-Functionalized Single-Walled Carbon Nanotube Chemiresistive Sensor Arrays.

In the CMOS integrated circuit implementation, the conductometric based readout circuit is designed and fabricated in 0.35um CMOS process. The individual

components include the op-amp and a 16:1 analog multiplexer. The op-amp is a three stage amplifier to provide a high gain and high output voltage swing. The op-amp achieves a 118.3 dB gain and 59.73 degrees phase margin. The analog multiplexer is realized using sixteen transmission gate switches and a 4:16 decoder logic circuit. The PAD size is 81.4um × 81.4um. The total area of the proposed readout circuit is 185um × 2300um. The circuit DC response for input resistance range of 10KΩ to 100KΩ gives a linear output voltage range from 1.016V to 0.101V and is linear. The circuit consumes 5.1mW of power. The conductometric readout circuit is proved to have portability and real time monitoring of the toxic substances in the environment and with the help of on-the-go USB communication protocol the data can be transferred into a host for further processing of the information.

For future work, it is intended to integrate the CMOS integrated readout circuit with the Porphyrin-Functionalized Single-Walled Carbon Nanotube Chemiresistive Sensor Arrays to form a more compact, cheaper, low power and increased portability solution to existing methods of commercially available environmental toxic substance monitoring products.

References

[1] US EPA, 1999. *Compendium Method TO-15, Determination o f Volatile Organic Compounds (VOCs) in Air Collected in Specially-Prepared Canisters and Analyzed by Gas Chromatograpy/Mass Spectrometry (GC/MS).* EPA/625/R-96/010b, Cincinnati, OH.

[2] Rothweiler, H., Schlatter, C., 1993. Human exposure to volatile organic-compounds in indoor air - a health risk. *Toxicological and Environmental Chemistry* 40: 93-102.

[3] Jia, C. (2007). *Volatile organic compounds in industrial, urban, and suburban areas: Sources and exposures.* (Order No. 3276194, University of Michigan). *ProQuest Dissertations and Theses,* 226

[4] Gordon, S. M., et al. "Volatile organic compounds in exhaled air from patients with lung cancer." *Clinical chemistry* 31.8 (1985): 1278-1282.

[5] Finlayson-Pitts, Barbara J., and James N. Pitts. "Tropospheric air pollution: ozone, airborne toxics, polycyclic aromatic hydrocarbons, and particles."*Science* 276.5315 (1997): 1045-1051.

[6] Cao, Wenqing, and Yixiang Duan. "Breath analysis: potential for clinical diagnosis and exposure assessment." *Clinical Chemistry* 52.5 (2006): 800-811.

[7] Ho, Clifford K., et al. "Review of chemical sensors for in-situ monitoring of volatile contaminants." *Sandia Report SAND2001-0643. Sandia National Laboratories, Albuquerque, NM* (2001).

[8] Guth, Ulrich, Winfried Vonau, and Jens Zosel. "TOPICAL REVIEW: Recent developments in electrochemical sensor application and technology---a review."*Measurement Science and Technology* 20.4 (2009): 2002.

[9] Shirsat, M. D., Sarkar, T., Kakoullis Jr, J., Myung, N. V., Konnanath, B., Spanias, A., & Mulchandani, A. (2012). Porphyrin-functionalized single-walled carbon nanotube chemiresistive sensor arrays for VOCs. *The Journal of Physical Chemistry C*, *116*(5), 3845-3850.

[10] Gründler, Peter. *Chemical sensors: an introduction for scientists and engineers*. Springer, 2007.

[11] Sekhar, Praveen K., et al. "Chemical sensors for environmental monitoring and homeland security." *The Electrochemical Society Interface* 19.4 (2010): 35.

[12] Myasoedov, B. F. "Chemical sensors (review)." *Bulletin of the Russian Academy of Sciences, Division of chemical science* 41.3 (1992): 383-387.

[13] Stetter, Joseph R., and William R. Penrose. "Understanding Chemical Sensors and Chemical Sensor Arrays (Electronic Noses): Past, Present, and Future."*Sensors update* 10.1 (2002): 189.

[14] Hanrahan, Grady, Deepa G. Patil, and Joseph Wang. "Electrochemical sensors for environmental monitoring: design, development and applications." *Journal of Environmental Monitoring* 6.8 (2004): 657-664.

[15] Eggins, Brian R. *Chemical sensors and biosensors*. Vol. 28. Wiley. com, 2008.

[16] A. J. Bard and L. R. Faulkner, *Electrochemical Methods: Fundamentals and Applications*. Wiley, 2001

[17] Janata, J. (Ed.). (2009). *Principles of chemical sensors*. Springer.

[18] Cho, Taeg Sang, et al. "The design of a low power carbon nanotube chemical sensor system." Proceedings of the 45th annual Design Automation Conference. ACM, 2008.

[19] Cho, Taeg Sang, et al. "A low power carbon nanotube chemical sensor system." Custom Integrated Circuits Conference, 2007. CICC'07. IEEE. IEEE, 2007.

[20] Kim, Hyun Tae. *A CMOS Analog Front-End IC for Gas Sensors*. Diss. Arizona State University, 2011.

[21] Penza, M., et al. "Pt-modified carbon nanotube networked layers for enhanced gas microsensors." Thin Solid Films 520.3 (2011): 959-965.

[22] Kanoun, Olfa, and Zied Fahem. "Potential of carbon nanotubes for sensor applications." Systems, Signals and Devices, 2008. IEEE SSD 2008. 5th International Multi-Conference on. IEEE, 2008.

[23] C. A. Thomas Jr, P.A. Springer, G.E. Loeb, Y. Berwald-Netter and L.M. Okun, "A miniature microelectrode array to monitor the bioelectric activity of cultured cells", Exp.Cell R., Vol. 74, pp. 61-66, Sep 1972.

[24] T. S. Cho, K.-J. Lee, J. Kong, and A. Chandrakasan, "A 32 μW 1.83-kS/s Carbon Nanotube Chemical Sensor System", IEEE Journal of Solid-State Circuits, Vol. 44, No. 2, Feb 2009.

[25] McEuen, Paul L., Michael S. Fuhrer, and Hongkun Park. "Single-walled carbon nanotube electronics." Nanotechnology, IEEE Transactions on 1.1 (2002): 78-85.

[26] Li, Jing, et al. "Carbon nanotube sensors for gas and organic vapor detection."Nano Letters 3.7 (2003): 929-933.

[27] Biesaga, Magdalena, Krystyna Pyrzyńska, and Marek Trojanowicz. "Porphyrins in analytical chemistry. A review." Talanta 51.2 (2000): 209-224.

[28] Zhang, Suyi, et al. "Molecular interactions of dimethyl methylphosphonate (DMMP) with metalloporphyrins: Determination of the binding mechanism by spectroscopic methods." Spectrochimica Acta Part A: Molecular and Biomolecular Spectroscopy 88 (2012): 137-143.

[29] Rahman, GM Aminur, et al. "Electronically interacting single wall carbon nanotube–porphyrin nanohybrids." Journal of Materials Chemistry 16.1 (2006): 62-65.

[30] S. S. Taylor and T. P. Thomas, “A 2pA/ radic;Hz 622 Mb/s GaAs MESFET transimpedance amplifier,” in *Solid-State Circuits Conference, 1994. Digest of Technical Papers. 41st ISSCC., 1994 IEEE International*, 1994, pp. 254–255.

[31] K. Iniewski, *VLSI Circuits for Biomedical Applications*. Artech House, 2008.

[32] B. Razavi, “A 622 Mb/s 4.5 pA/ radic;Hz CMOS transimpedance amplifier [for optical receiver front-end],” in *Solid-State Circuits Conference, 2000. Digest of Technical Papers. ISSCC. 2000 IEEE International*, 2000, pp. 162–163, 453.

[33] Jichun Zhang, N. Trombly, and A. Mason, “A low noise readout circuit for integrated electrochemical biosensor arrays,” in *Proceedings of IEEE Sensors, 2004*, 2004, pp. 36– 39 vol.1.

[34] Jichun Zhang, Yue Huang, N. Trombly, Chao Yang, and A. Mason, “Electrochemical array microsystem with integrated potentiostat,” in *2005 IEEE Sensors*, 2005.

[35] Afridi, M. Y., et al. "Implementation of CMOS compatible conductance-based micro-gas-sensor system." *European Conference on Circuit Theory and Design, pp.(III)*. 2001.

Biographical Information

Sujith Dermal is a candidate for the Master of Science in Electrical Engineering at The University of Texas at Arlington. He received his Bachelor's degree in Electronics and Communication Engineering from Cochin University of Science and Technology, India. He worked as Hardware Engineer at HCL Technologies, India prior joining for his MS at UT Arlington. He joined the AMIC Design Lab and started his Master's thesis work under the supervision of Dr. Sungyong Jung in Fall 2011. His interests include Analog/Mixed Signal integrated circuits and systems. Currently he is working as an Analog and Mixed Signal IC Validation Engineer at Freescale Semiconductor, AZ.